End-to-end flood risk assessment: A coupled model cascade with uncertainty estimation

McMillan, Hilary K.; Brasington, James

Published in:
Water Resources Research

DOI:
10.1029/2007WR005995

Publication date:
2008

Citation for published version (APA):
McMillan, H. K., & Brasington, J. (2008). End-to-end flood risk assessment: A coupled model cascade with uncertainty estimation. *Water Resources Research*, *44*. https://doi.org/10.1029/2007WR005995

End-to-end flood risk assessment: A coupled model cascade with uncertainty estimation

Hilary K. McMillan[1] and James Brasington[2]

Received 26 February 2007; revised 23 October 2007; accepted 10 December 2007; published 18 March 2008.

[1] This paper presents the case for an 'End-to-End' flood inundation modeling strategy: the creation of a coupled system of models to allow continuous simulation methodology to be used to predict the magnitude and simulate the effects of high return period flood events. The framework brings together the best in current thinking on reduced complexity modeling to formulate an efficient, process-based methodology which meets the needs of today's flood mitigation strategies. The model chain is subject to stochasticity and parameter uncertainty, and integral methods to allow the propagation and quantification of uncertainty are essential in order to produce robust estimates of flood risk. Results from an experimental application are considered in terms of their implications for successful floodplain management, and compared against the deterministic methodology more commonly in use for flood risk assessment applications. The provenance of predictive uncertainty is also considered in order to identify those areas where future effort in terms of data collection or model refinement might best be directed in order to narrow prediction bounds and produce a more precise forecast.

Citation: McMillan, H. K., and J. Brasington (2008), End-to-end flood risk assessment: A coupled model cascade with uncertainty estimation, *Water Resour. Res.*, *44*, W03419, doi:10.1029/2007WR005995.

1. Introduction

1.1. Modern Responses to Flood Risk

[2] In recent years, significant changes in scientific, public and government opinion have brought about a reappraisal of flood management policy in Britain. Costly failures of structural flood defense measures have highlighted the inadequacy of historical designs when faced with the changing nature of river flow characteristics due to climate change, urbanization and land-use change on floodplains. This has been matched by a broadening of the concept of flood risk assessment from purely economic considerations to cover wider social and environmental values [*DEFRA*, 2002]. In response to these drivers, current governmental policies on flood prevention and mitigation measures increasingly favor 'soft' solutions centering on the restoration, enhancement or creation of the natural functions of the floodplain, over 'hard' engineering solutions.

1.2. The Need for an Updated Approach to Flood Risk Assessment

1.2.1. Non-Stationarity of the Flood Generation Process

[3] Today we are in a period of what is widely considered to be enhanced flood risk caused by the joint human factors of climate change and land-use change [*Wheater*, 2006]. Non-stationarity is exhibited in the recent precipitation record [*Dai et al.*, 1997; *Easterling et al.*, 2000; *Groisman et al.*, 2004; *Huntington*, 2006; *Osborn and Hulme*, 2002; *Staeger et al.*, 2003], suggesting an intensification of the hydrological cycle, and giving credence to GCM model predictions of increased frequency of heavy rainfall events [*Arnell et al.*, 2001; *Arnell and Reynard*, 1996]. These results may be compounded by aspects of land-use change which reduce the ability of catchments to store flood water and to attenuate flood peaks.

[4] If non-stationarity is accepted as existing in the flood generation process, this violates a critical assumption of the mathematical theory behind conventional, statistical flood risk assessment. In order to derive the extreme value distribution which these methods fit to a data series of recorded flood peaks, floods must be assumed to occur as independent, identically distributed, random events from a single, stationary distribution. Even where recurrence intervals are regularly updated with new data, the non-stationarity of the process over the data collection period invalidates that assumption.

1.2.2. Distributed Flood Risk Mapping

[5] Historically, the chief focus of flood risk assessment (FRA) has been the derivation of discharge or stage for a given set of return periods, reflecting a reliance on structural flood defense works whose aim was to contain flood flows within the designated channel. Soft engineering solutions, floodplain restoration and homeowner responsibility demand instead spatially distributed flood risk information. To cater for this demand, 1D hydraulic models are typically extended to provide 'basin-fill' water elevation mapping using either extended cross-sectional data or a network of floodplain storage cells [e.g., *USACE*, 2005]. This method typifies a more simplistic view of the floodplain as purely a storage reservoir.

[1]National Institute of Water and Atmospheric Research Ltd, Riccarton, Christchurch, New Zealand.
[2]Centre for Catchment and Coastal Research, University of Wales, Aberystwyth, UK.

0043-1397/08/2007WR005995

[6] In contrast, flood defense circumvention or failure during extreme events has demonstrated the connectivity of channel and floodplain as a coupled system during times of flood. The hydraulic approximations made by a 1D model prevent representation of lateral momentum transfer between the river and the floodplain, and cannot account for the pressure gradients which force water flows at highly variable rates between the two areas. The increased expectation of flood flows through complex urban areas, due to changes in flood defense strategy, requires flood risk mapping based on 2D models which are capable of providing a dynamic representation of water transport onto and around the floodplain.

2. Development of a Process-Based Continuous Simulation Methodology

[7] This paper proposes a preliminary structure for a modern FRA methodology which, motivated by a desire to address the deficiencies in standard FRA techniques outlined above, seeks to combine the benefits of the latest modeling techniques to produce an efficient, integrated approach to current FRA requirements. A central aim for the structure was that it should embody a process-based approach; this greatly increases the predictive power of the system in response to novel input and boundary conditions and allows the structure and parameters of the system to be modified to reflect knowledge of changing conditions of climate and land-use. In order to achieve this, the FRA structure is underpinned by the technique of continuous simulation.

[8] Continuous simulation uses the available precipitation record for the catchment as a basis for creation of long synthetic rainfall series. These series are used as input to a rainfall-runoff model to produce the corresponding discharge series, from which extreme event frequencies may be calculated explicitly. The method provides continuous soil moisture accounting which gives implicit consideration of antecedent wetness conditions in the catchment. Using this flexible method, climate change might be represented via a modification of the rainfall frequency distributions using estimates of the effects of climate change on particular aspects of rainfall patterns. Land-use change could be included via a modification of the rainfall-runoff model structure or parameters, such as an increase in runoff coefficient. Although continuous simulation has previously been used to forecast the discharge magnitude of extreme floods [*Cameron et al.*, 1999; *Chetty and Smithers*, 2005; *Franchini et al.*, 2000; *Hashemi et al.*, 2000; *Maskey et al.*, 2004; *Onof et al.*, 1996; *Pandit and Gopalakrishnan*, 1996], and in rare cases extended to applications in design of structural floodplain defense measures [*Hsieh et al.*, 2006] and flood mapping studies [*Faulkner and Wass*, 2005], it has not been considered suitable for integration into the standard FRA framework due to the computational overhead required. However, by using a relatively simple rainfall-runoff model, it proves to be a practical and valuable tool.

[9] The new structure is also defined by its integrated, 'End-to-End' approach to FRA. As management plans become catchment- or basin-wide in their scope, so too should FRA methods be spatially and temporally ambitious. No part of the catchment a isolation; the process-based approach attempts to replicate the connected system through a cascade of coupled models representing precipitation regime, rainfall-runoff characteristics and floodplain inundation behavior. Discharge estimates from the continuous simulation of runoff are used to drive a 2D model of floodplain hydraulics which utilizes new, high-resolution elevation data to enable urban floodplain modeling at the smallest scales and paves the way for additional modules for vulnerability and damage assessment. These would be used to calculate the social and economic impacts of floods, for example using information on building use or value [*Apel et al.*, 2004; *Merz et al.*, 2004], and could be implemented within a risk-based sampling technique to reduce computational burden [*Dawson et al.*, 2005]. Finally, the coupled model structure may be run within a proven uncertainty estimation framework, to allow explicit calculation of the cascading uncertainties.

[10] This technique has previously been tested within a reduced stochastic-rainfall-model: rainfall-runoff-model system [*Blazkova and Beven*, 2002, 2004; *Cameron et al.*, 2000; *Kuchment and Gelfan*, 2002; *Lamb*, 1999]. Uncertainty estimation within a full 'End-to-End' approach is already being successfully applied to event-based simulation [*De Roo et al.*, 2003; *Pappenberger et al.*, 2005; *Sattler and Feddersen*, 2005], although these authors note the computational limitations currently placed on the method. This study places particular emphasis on the need to integrate uncertainty estimates into model predictions targeted for end-user communities.

3. Modeling and Methods

3.1. Overview

[11] A coupled model chain is created consisting of a stochastic rainfall model, a rainfall-runoff model and a floodplain inundation model. This section presents an outline of each model, followed by the coupling methodology. Component models are chosen to represent the latest advances in reduced-complexity methods, however flexibility is key to the End-to-End FRA ethos and models could be varied according to individual case attributes.

[12] The model descriptions given here are necessarily brief; full detail may be found in *McMillan* [2006] and *McMillan and Brasington* [2007].

3.2. Component Models

3.2.1. Stochastic Rainfall Model

[13] All stochastic rainfall generation models rely on an initial decomposition of rainfall records to identify frequency characteristics of storm data (e.g., depth, duration and intensity), which are then used to parameterize a rainfall generation mechanism. A profile-based method was chosen, for ease of implementation and a desire to reduce the need for parameterization by use of a 'data based' method. The method splits the total storm depth into time step depths by using a profile or mass curve [e.g., *Arnaud and Lavabre*, 1999; *Beven*, 1987; *Blazkova and Beven*, 2002; *Cadavid et al.*, 1991; *Cameron et al.* 1999; 2000; *Cernesson et al.*, 1996; *Diaz-Granados et al.*, 1984; *Eagleson*, 1972; *Hebson and Wood*, 1982].

[14] The distributions of storm intensity, duration and inter-arrival time are collated and smoothed using Gaussian kernel density estimation [*Silverman*, 1982, 1986; *Antoniadis*,

1995], with modifications made for skewed or discontinuous distributions as appropriate. In order to create the stochastic storm sequence, random samples were drawn from these distributions, and a storm created using a profile drawn randomly from the storm record. Two modifications were made to this basic model structure to improve model performance, as follows.

[15] First, storms may be segregated by season if characteristic differences exist [e.g., *Blazkova and Beven*, 2002; *Walshaw*, 1994]. Here a split into two seasons was made (February-August, September-January) to reflect seasonality in rainfall totals. Secondly, the storm characteristics showed a negative correlation between intensity and duration, which should be recognized within the model structure to optimize performance [*Cameron et al.*, 1999; 2000; *Goel et al.*, 2000; *Kurothe et al.*, 1997]. The empirical intensity distributions were therefore split by duration into 5 classes before sampling, this method being chosen in preference to the use of a bivariate intensity-duration sampling distribution to avoid limitation of model stochasticity. An additional modification to extend the tail of the intensity distributions using a fitted extreme value distribution, in order to accommodate the possibility of more intense events than those in the recorded sequence, was rejected after trials showed that it caused overestimation of observed maximum rainfalls.

3.2.2. Rainfall-Runoff Model

[16] A transfer function methodology was chosen to provide the rainfall-runoff component of the model chain. This popular class of models originates from unit hydrograph theory and the Nash Cascade [*Nash*, 1959], and represents the catchment as a linear system of interconnected flow pathways, modified by a nonlinear transform to represent runoff generation. This model type combines the benefits and well-conditioned nature of a lumped model while allowing knowledge of catchment structure to be incorporated into model definition. Various versions of this model have been implemented [e.g., *Jakeman et al.*, 1990; *Young and Beven*, 1991, 1994 and a comprehensive review by *Young*, 2003]; the version described by *Sefton and Howarth* [1998] was used here.

[17] The equations governing the non-linear rainfall transform are as follows:

$$u_t = R_t(S_t + S_{t-1})/2 \tag{1}$$

$$S_t = cR_t + \left[1 - \frac{1}{\tau(T_i)}\right] S_{t-1} \tag{2}$$

$$\tau(T_i) = \tau_w \cdot \exp(20f - T_i f) \tag{3}$$

Where u_t is the volume of effective rainfall at time t resulting from input rainfall R_t. S_t represents the catchment storage index at time t, $\tau(T_i)$ is the recession rate of S_t at temperature T_i which depends on the recession rate at 20°C, τ_w. The parameter c ensures equality of effective rainfall and runoff volumes. Parameter f modulates evapotranspiration with temperature, requiring an input temperature series.

[18] The linear routing module of the rainfall-runoff model uses a transfer function to convert effective rainfall u_t into flow Q_t. The most usual form of transfer function to be specified for small catchments consists of two parallel pathways representing quickflow and slowflow. This choice of model structure was accepted for the study catchment, after consideration of physical catchment characteristics and gauging carried out in the field, together with model trials. The model structure is shown in equation (4).

$$Q_t = \frac{b_0 + b_1 \cdot z^{-1}}{1 - a_1 \cdot z^{-1} - a_2 \cdot z^{-2}} \cdot u_{t-\delta} = \left[\frac{\beta_q}{1 - \alpha_q \cdot z^{-1}} + \frac{\beta_s}{1 - \alpha_s \cdot z^{-1}}\right] \cdot u_{t-\delta} \tag{4}$$

Equation (4): *Two-component transfer function structure*

Where z^{-1} is the backward shift operator, i.e., $z^{-1}Q_t = Q_{t-1}$. The parameters that must be estimated are β_q, β_s, α_q, α_s, δ (where suffix q represents quickflow parameters, s represents slowflow parameters), given calibration data consisting of effective rainfalls $\{u_t\}$ and flows $\{Q_t\}$. The parameters for both non-linear and linear model parts are estimated using the GLUE procedure [*Beven and Binley*, 1992] outlined below.

3.2.3. Floodplain Inundation Model

[19] The floodplain inundation model chosen for this application takes advantage of significant recent progress in reduced complexity modeling, achieved by directly coupling 1d channel hydraulic models with 2d raster storage cell approximation for floodplain flows [e.g., *Bates and De Roo*, 2000]. This approach offers order of magnitude gains in computational efficiency over more complex finite element and volume codes [*Aronica et al.*, 2002; *Horritt and Bates*, 2001].

[20] The channel model uses the kinematic approximation to the Saint-Venant equations, which describe one-dimensional unsteady open channel flow. They consist of a continuity equation and a momentum equation (equations (5) and (6)). Variables used are: Q, flow; A, cross-sectional area; t, time; x, horizontal position; y, vertical position; g, gravity; S_0, bed slope; S_f, friction slope.

$$\text{Continuity Equation :} \quad \frac{\partial Q}{\partial x} + \frac{\partial A}{\partial t} = 0 \tag{5}$$

$$\text{Momentum Equation :} \quad \underbrace{\frac{1}{A} \cdot \frac{\partial Q}{\partial t}}_{\substack{\text{Local}\\ \text{Acceleration}\\ \text{Term}}} + \underbrace{\frac{1}{A} \cdot \frac{\partial}{\partial x}\left(\frac{Q^2}{A}\right)}_{\substack{\text{Convective}\\ \text{Acceleration}\\ \text{Term}}} + \underbrace{g\frac{\partial y}{\partial x}}_{\substack{\text{Pressure}\\ \text{Force}\\ \text{Term}}} \underbrace{-g(S_0}_{\substack{\text{Gravity}\\ \text{Force}\\ \text{Term}}} \underbrace{-S_f)}_{\substack{\text{Friction}\\ \text{Force}\\ \text{Term}}} = 0 \tag{6}$$

The kinematic approximation uses the full continuity equation, but only the gravity and friction force terms in the momentum equation, neglecting pressure and acceleration terms.

[21] The floodplain model uses a raster cell approach that has been popularized by *Bates and De Roo* [2000] and *De Roo et al.* [2000] with their model LISFLOOD-FP; similar ideas have also been used by *Estrela and Quintas* [1994] and *Romanowicz et al.* [1996], all building on methods suggested by *Cunge et al.* [1976]. The model uses numerical discretization in space and time, as with the channel model.

The floodplain is treated as a grid of square cells, with flow allowed between 4-connected cells. As in the channel model, continuity and momentum equations are solved to calculate flow rates. The continuity equation relates flow across cell boundaries to the volume stored in the cell (equation (7)); the momentum equation uses Manning's Law to relate flux to surface slope and hydraulic radius (equation (8)).

$$\text{Continuity Equation}: \quad \frac{\partial h^{i,j}}{\partial t} = \frac{Q_x^{i-1,j} - Q_x^{i,j} + Q_y^{i,j-1} - Q_{y\,y}^{i,j}}{\Delta x \Delta y} \tag{7}$$

$$\text{Momentum Equation}: \quad Q_x^{i,j} = \frac{h_{flow}^{5/3}}{n}\left(\frac{h^{i-1,j} - h^{i,j}}{\Delta x}\right)\Delta y \tag{8}$$

Where $h^{i,j}$ is water depth at cell (i, j), h_{flow} is free water depth between two cells, Δx and Δy are the cell dimensions, n is Manning's friction coefficient, and Q_x and Q_y are the flow rates in two directions between cells.

[22] Two major modifications are made to this basic model structure; both are described more fully by *McMillan and Brasington* [2007]. First, the numerical stability of the model is improved using a redesigned function to limit excessive flows between cells, which occur particularly in areas of deep, ponded water due to the use of numerical approximations to the governing differential equations. This limiter aimed to improve on that designed by *Hunter et al.* [2004], by recognizing the interaction of multidirectional flow paths and hence retaining information on preferential flow pathways within the floodplain. This was achieved by imposing a total outflow limit on each cell to be split proportionally between the multiple outflows; implicitly considering these flows as dependant processes. The limiter form is shown in equation (9). The use of a limiter removes model sensitivity to floodplain friction, a pattern previously noted in storage cells models, and arises because the form of the flow limiter becomes the dominant control on floodplain flows [*Romanowicz and Beven*, 2003; *Hunter et al.*, 2004; *Hall et al.*, 2005].

$$Q_x^{i,j} = \min\left\{ Q_x^{i,j}, \underbrace{\left(\frac{Q_x^{i,j}}{Q_x^{i,j} + Q_x^{i-1,j} + Q_y^{i,j} + Q_y^{1,j-1}}\right)}_{\text{Proportion of flow}} \cdot \underbrace{\left(\frac{\min\left\{H_x^{i,j}, H_x^{i-1,j}, H_y^{i,j}, H_y^{i-1,j}\right\}\Delta x \Delta y}{1 + 1/(Number \cdot of \cdot Outflows)}\right)}_{\text{Max total outflow before surface gradient is reversed}}, \underbrace{\left(\frac{Q_x^{i,j} \cdot h^{i,j} \cdot \Delta x \Delta y}{\left(Q_x^{i,j} + Q_x^{i-1,j} + Q_y^{i,j} + Q_y^{1,j-1}\right) \cdot \delta t}\right)}_{\text{Outflow required to empty cell}} \right\} \tag{9}$$

Secondly, the model is upgraded to allow sub-grid model parameterization, in an attempt to harness the wealth of terrain information contained within a LIDAR scan of a river reach within an efficient model structure. This is achieved by using the concept of 'cell porosity' to allow the use of sub-grid topographic information within a coarse resolution model. The porosity function quantifies the percentage of the assumed cell volume that is available for water storage after accounting for sub-grid features; similarly modified values of cell boundary cross-section area and wetted perimeter are also defined. By using this information to adjust the continuity and momentum equations, model behavior may react to preferential flow directions and flow volumes in a way that is not possible using a simple roughness coefficient. The method is designed to reflect the first order controls on flow conveyance while enabling simulations to be carried out at a computationally efficient resolution; *Yu and Lane* [2006] demonstrate the potential of the concept by using sub-grid scale information at a resolution half that of the model.

3.3. Model Coupling

3.3.1. Using GLUE in End-to-End Hydrological Modeling

[23] The GLUE technique [*Beven and Binley*, 1992] is a tool for investigation of model response and associated uncertainty, under equifinality of model structure or parameterization. On the basis of principles from Bayesian statistics, the technique relies on the computation of a 'likelihood' measure, an estimate of how likely the model is to produce acceptable simulations based on its performance tested against some observed data. The model is run many times using many different parameter sets (often chosen using Monte Carlo analysis), and the predictions of each behavioral model are weighted using a normalized likelihood value. A cumulative distribution can then be calculated for each prediction variable at each timestep, and hence quantiles as required (equation (10)).

$$P(Q_t < q) = \sum\nolimits_{i \in X} L(\Theta_i) \text{ where } X = \left\{ i | Q_t^i < q \right\} \tag{10}$$

Where Q_t is the predicted flow (or other variable) at time t, q is the observed flow, Θ_i is the ith set of parameters for the model, $L(\Theta_i)$ is the likelihood value obtained when the model is run using these parameters, and Q_t^i is the predicted flow at time t using these parameters. The advantages of the technique lie in the ability to make predictions of uncertainties in highly non-linear systems where the assumptions of traditional statistical techniques prove too restrictive.

[24] It is important to note that when estimating confidence limits using GLUE, the discharge predictions at each timestep do not relate to a single set of parameter values and hence a single model realization. Thus when applying GLUE to coupled models, uncertainty bounds cannot be cascaded through the model series by treating the bounds for output time series as a prediction relating to a single parameter set that may be input into the following model. Instead, results relating to each parameter set must be propagated through the model chain individually, the resulting computational demands presenting serious constraints on the number of dimensions over which uncertainty can be considered. Decisions therefore had to be made in order to restrict the scope of the analysis, balancing the efficiency of the system against the extent and accuracy of the results.

3.3.2. Coupling of Rainfall and Rainfall-Runoff Models

[25] The rainfall simulation model was derived using empirical data rather than fitted parameters, and therefore there is no explicit parameter uncertainty. Instead, the perceived uncertainty in a rainfall simulation relates to the choice of model type and the inherent stochasticity of the model; one realization of a rainfall series represents only a single possible outcome. We therefore consider the uncertainty in realization of rainfall series, together with the uncertainty of choice of rainfall-runoff model parameters. Model structural uncertainty is not considered here, although it is inherent in the choice of each component model.

[26] Although the most comprehensive approach to uncertainty estimation would be to search these two sources of uncertainty as a 2D parameter space (i.e., every rainfall realization coupled with every parameter set), this strategy would be extremely costly in computational terms. Instead, following *Cameron et al.* [1999], independent random selections are made from the two sets, and this joint Monte Carlo sample assigned a performance weighting from the rainfall-runoff model parameter set since the weightings of the rainfall simulations are deemed equal.

3.3.3. Coupling of Rainfall-Runoff and Floodplain Hydraulic Models

[27] The rainfall-runoff model is used to process each series of simulated rainfall to yield an estimate of channel discharge at the upstream boundary of the inundation model. The models must be coupled in such a way as to allow the uncertainty in discharge series to be represented in the input to the floodplain hydraulic model; the aim being to achieve inundation extent estimation at various return periods, while specifying the uncertainty associated with the predictions. The most complete technique for estimating this uncertainty would be to route the discharge predicted by each rainfall simulation/rainfall-runoff model combination through the floodplain hydraulic model. Unfortunately this is clearly not a practical proposition due to computation restrictions.

[28] However, by careful choice of assumptions with regard to the flow behavior at the site, efficient methods for estimation of inundation frequency are possible. Here, an approach based on three key assumptions is proposed.

[29] • First, it is assumed that the inundation extent related to a particular flow event is independent of flow conditions prior to the time at which out-of-bank flow began. This is justified due to the rarity of closely spaced flood events, and allows modeling of individual events to replace the need for continuous simulation.

[30] • Secondly, it is assumed that the frequency distribution of inundation extent may be characterized using an annual maximum series for flow events, rather than requiring a peaks-over-threshold (POT) analysis. This is a reasonable assumption given a long simulated data series: *Robson and Reed* [1999] show that the advantage gained by using POT data can typically be acquired using one additional year of annual maximum data.

[31] • A third assumption is made that the event in each year which causes the greatest inundation is that which has the greatest instantaneous peak discharge. This is based on the premise that the magnitude of an event is a good indication of other damaging attributes of a flood such as over-bank volume or duration (the strong peak flow: volume relationship found in the test catchment is described in the results section). This assumption is key to reducing processing time as the storm with maximum discharge in each hydrological year can be easily identified. In contrast, identifying the storm causing most inundation from a flow series would be a challenging and time-consuming task, and might not be possible without carrying out the inundation simulation in full.

[32] A final decision was taken that uncertainty in calibration of the floodplain model, i.e., value of Manning's n for channel friction, would not be part of the coupled uncertainty analysis. If this were to be undertaken, then for each return period of interest, the design event corresponding to each discharge series realization would have to be propagated through the inundation model with each possible value of channel friction, giving rise to tens of thousands of simulations. This is not computationally feasible given that each inundation simulation takes several hours to perform (235 min benchmarked on a Pentium 4, 3.2 MHz PC with 1.5GB RAM, based on simulations with the optimal channel friction coefficient, $n = 0.05\ m^{-1/3}s$). Instead, by considering only the uncertainty from the rainfall and rainfall-runoff models, the confidence bounds on the design event magnitude may be translated directly into confidence bounds on inundation extent. A limited sensitivity analysis of the model response to uncertainty in channel friction is, however, undertaken to provide a gauge of its relative effects on the inundation predictions. There is clear scope for this additional uncertainty source to be more fully considered; however at present this simplified analysis is thought reasonable as unlike the strongly equifinal behavior of the rainfall-runoff model, the hydraulic model calibration showed a unimodal performance distribution with a single optimal value when validated against combined inundation and hydrograph data.

3.3.4. Process Methodology

[33] Drawing on the assumptions outlined above, the process methodology may thus be described. Simulated rainfall series, of a length appropriate to the design event to be estimated, are produced using the stochastic rainfall model. One series is generated to correspond to each rainfall-runoff model parameter set, the number of which must be chosen by the investigator. These sets are randomly created by sampling from the feasible parameter ranges. Each set is assigned a performance ('likelihood') value corresponding to its ability to correctly reproduce a flow record. In the test application described below, the parameter sets are validated using an 15-year rainfall-flow record. The fit between observed and predicted flow is tested using the R^2 criterion [*Nash and Sutcliffe*, 1970], and the parameter set is rejected for values <0.6.

[34] Each rainfall series is routed through the rainfall-runoff model run with the corresponding parameter set. On completion of this step, a set of T-year discharge estimates is therefore available by reading directly from a listing of the maximum flow in each simulated year. For each rank position in the series, the set of possible realizations of discharge value is ordered and associated with the parameter set performance value. A weighted cumulative distribution of discharge for each of these return periods can therefore be created, and upper and lower limits at the required confidence level together with any other quantiles produced by interpolation.

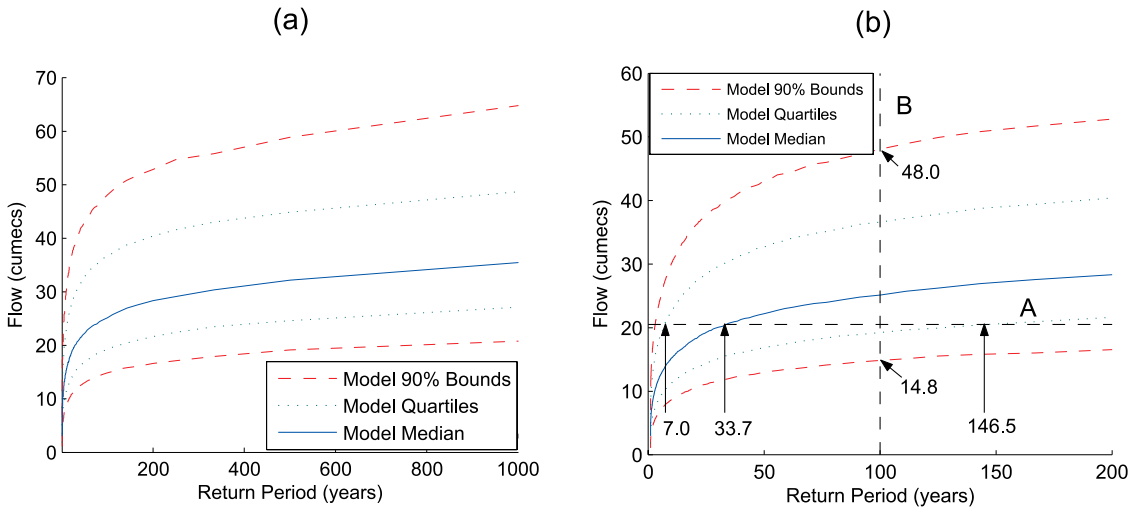

Figure 1. Modeled Discharge: Return Period Relation. (a) Full Range. (b) Detail. Dashed Lines show A. Discharge associated with 2001 flood, with return period estimated from median and quartiles and B. Discharge associated with 100-year flood.

[35] The discharge alone is insufficient to create the flow hydrograph required for input into the floodplain inundation model. The hydrograph is therefore produced using a triangular approximation, based on an empirical flow-volume relationship derived for the catchment, together with standard percentages of flow volume before and after the peak. Trials showed that this method was effective in providing accurate estimation of flood volumes.

4. Test Application: Upper Granta Catchment

[36] This section sets out a trial application of the end-to-end forecasting methodology, based on a 2 km reach of the River Granta in Cambridgeshire, UK, which has a long history of flooding. Full details of the reach and catchment hydrology are presented by *McMillan* [2006]. The catchment is characterized by agricultural land with gentle gradients and lies on a chalk aquifer overlain by Boulder Clay. Channel widths through the study reach are typically 5–10 m with slopes in the order of 0.5% and thus within the appropriate limits for a kinematic approximation of channel hydraulics [*Woolhiser and Liggett*, 1967]. The study reach straddles the town of Linton which has been frequently affected by severe flooding, most recently during October 2001. In this event, flooding occurred when 90 mm of rain fell in 17 h onto an already raised water table and caused extensive damage to 72 properties, including key historic buildings in the town centre. Estimates of the return period for this event range from 100–400 years [*Halcrow*, 2004; *McMillan*, 2006]. Records from this event were used to parameterize the floodplain inundation model; 15-year rainfall and discharge records from the catchment were used to create the stochastic rainfall model and to assign performance values for each rainfall-runoff model parameter set. The aim of the trial was to allow inundation hazard mapping for long return-period events, and therefore rainfall series of 1000 years were used. These were then processed to obtain predictions of discharge at yearly return periods up to 1000 years, and inundation extent at a range of return periods: 10, 50, 100, 500 and 1000 years.

5. Results

5.1. Discharge Prediction

[37] The discharge series produced from the coupled stochastic rainfall and rainfall-runoff models were used to produce cumulative distributions of discharge, plotted in Figure 1A, and shown in detail in Figure 1B for comparison with the 2001 flood.

[38] The results demonstrate the high level of uncertainty associated with predictions made using the simulated rainfall series and rainfall-runoff model. For example, the 90% confidence interval for the 100-year flood discharge is 14.8–48.0 m^3s^{-1} (Figure 1B), a large uncertainty in terms of flood hazard or in the cost-benefit ratio of any flood protection works. Similarly, estimates the return period of the October 2001 flood (20.5 m^3 s^{-1}) range from 7 to 146 years between the 5% and 75% quartiles (the return period estimated from the upper 90% bound was not captured).

5.2. Hydrograph Formation

[39] The hydrograph for each return period (10, 50, 100, 500 and 1000 years) at the 5%, 50% (median) and 95% percentiles was formed according to the empirical flow-volume relationship found (equation (11)).

$$\text{Volume} = 36720 * \text{Flow}^{1.35} \tag{11}$$

Equation (11): *Regression Relationship between Peak Flow (m^3s^{-1}) and Volume (m^3)*

[40] The strong correlation found between flow and volume (correlation coefficient 0.90) justifies the use of a standardized hydrograph based on peak value. As an example, the hydrographs for the 1000-year flood are shown in Figure 2.

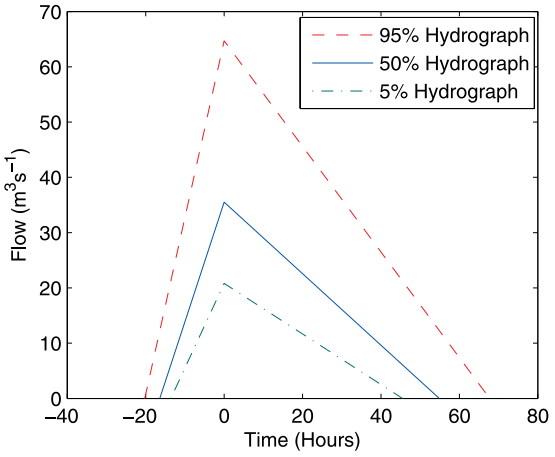

Figure 2. Design Hydrographs for the 1000-year return period, at the 5%, 50% and 95% points of the cumulative distribution.

5.3. Inundation Extent

[41] The design hydrographs give discharge series for the gauging station at Linton, upstream of the town centre, forming the upstream boundary condition for the hydraulic model. Following model evaluation, the floodplain code was implemented at 10 m resolution using the sub-grid porosity treatment for maximum computational efficiency. The channel friction coefficient (Manning's n) was set at 0.05 $m^{-1/3}s$, which gave optimal performance judged using a multicriteria validation for the 2001 flood event. This validation was based on a weighted combination of performance measures in hydrograph simulation and inundation behavior. Downstream hydrographs were judged according to accuracy of peak discharge magnitude and timing; inundation simulations were validated using a fuzzy performance measure which tested flood depth prediction for each inundation property, while allowing a margin of error for perceived reporting inaccuracies. For each return period, the hydraulic model was used to produce an inundation simulation relating to the design hydrographs for the 5%, 50% and 95% points of the distribution of peak discharge magnitudes. The results are shown in Figure 3.

5.4. Communication of Results

[42] The spatial pattern of inundation extent evident in Figure 3 is ultimately constrained by the valley morphology, so that despite large differences in the peak discharges of the extreme return periods, the maximal inundation envelope remains comparatively consistent. This is due to relatively steep topography at the natural boundaries of the floodplain which serves to constrain flood waters. However, it is also at this boundary that accuracy in prediction becomes more critical, as beyond the edge of the floodplain, density of housing increases dramatically. On the floodplain itself, there are few buildings, as waterlogged land and frequent flooding have constrained construction.

[43] This illustrates the importance of presenting results in a method sensitive to the intended use. Mapped inundation extents (Figure 3) would be useful for strategic and emergency planning at the local scale, e.g., preparation of emergency evacuation and traffic routing plans. However, for applications such as a benefit-cost analysis for a structural flood defense scheme, derived statistics such as number of houses flooded may present the trends more clearly (Figure 4). Further analysis could count only houses flooded beyond the protection limits of sandbags or removable floodgates.

[44] Figure 4 demonstrates a sharp rise in the number of properties flooded between the 10–100 year events; then a smaller increase up to the 1000-year event. This might suggest a threshold return period beyond which the expenditure involved in containing the Granta would not be realized in terms of damage saving. A worthwhile extension of the current work would be to link the properties in the area to a valuation, perhaps through zoning by postcode, in order to estimate the financial cost of each flood event. This could be achieved using depth-damage curves tailored to building type. Depth mapping would also be useful to aid identification of areas of high risk to life and greater damage to property. Calculated variables such as area and number of houses inundated could be used directly within the UK government system for assessment of future flood defense engineering works [*DEFRA*, 2002].

6. Constraining Uncertainty in End-to-End Modeling

6.1. Constraining Uncertainty in Discharge

[45] Quantifying the uncertainty in discharge prediction and analyzing its provenance offers the scope to determine the main sources of uncertainty, and identify means of uncertainty reduction through refinement of model structure, parameterization or boundary condition specification. Two example uncertainty sources are considered here.

6.1.1. Effects of Uncertainty in Rainfall Series

[46] Part of the uncertainty in discharge is due to the stochasticity of precipitation patterns that force the model chain, simulated here via the ensemble of 1000 climate scenarios. To consider the reduction in uncertainty if improved knowledge of future rainfall behavior was available, we simulate the extreme case where the full 1000-year rainfall series is known exactly. The Monte Carlo simulations are re-run using a single random 'correct' series, with each rainfall-runoff model parameter set as before (Figure 5).

[47] The return period-flow curves are less smooth than previous results, representing the increased dependence on model response to particular rainfall events. The 90% confidence bounds for the 100-year discharge are only slightly reduced, from [14.8, 48.0] to [14.8, 42.4] $m^3\ s^{-1}$ (Figure 5B), indicating that rainfall uncertainty has only a small impact on long term discharge prediction. However, the estimate of a particular quantity may be altered by a significant margin, e.g., the 2001 flood is estimated as having a return period of 47.4 years instead of 33.7. The limited effect of uncertainty in precipitation patterns however ultimately reflects the derivation of the rainfall model from a single 15-year gauged record. A longer rainfall series might contain implicit non-stationarity that exerts a significant control on discharge response.

6.1.2. Effects of Uncertainty in Rainfall-Runoff Model

[48] To test the effect of uncertainty in rainfall-runoff model parameterization, the suite of model simulations were rerun, using the original set of rainfall series, but the single

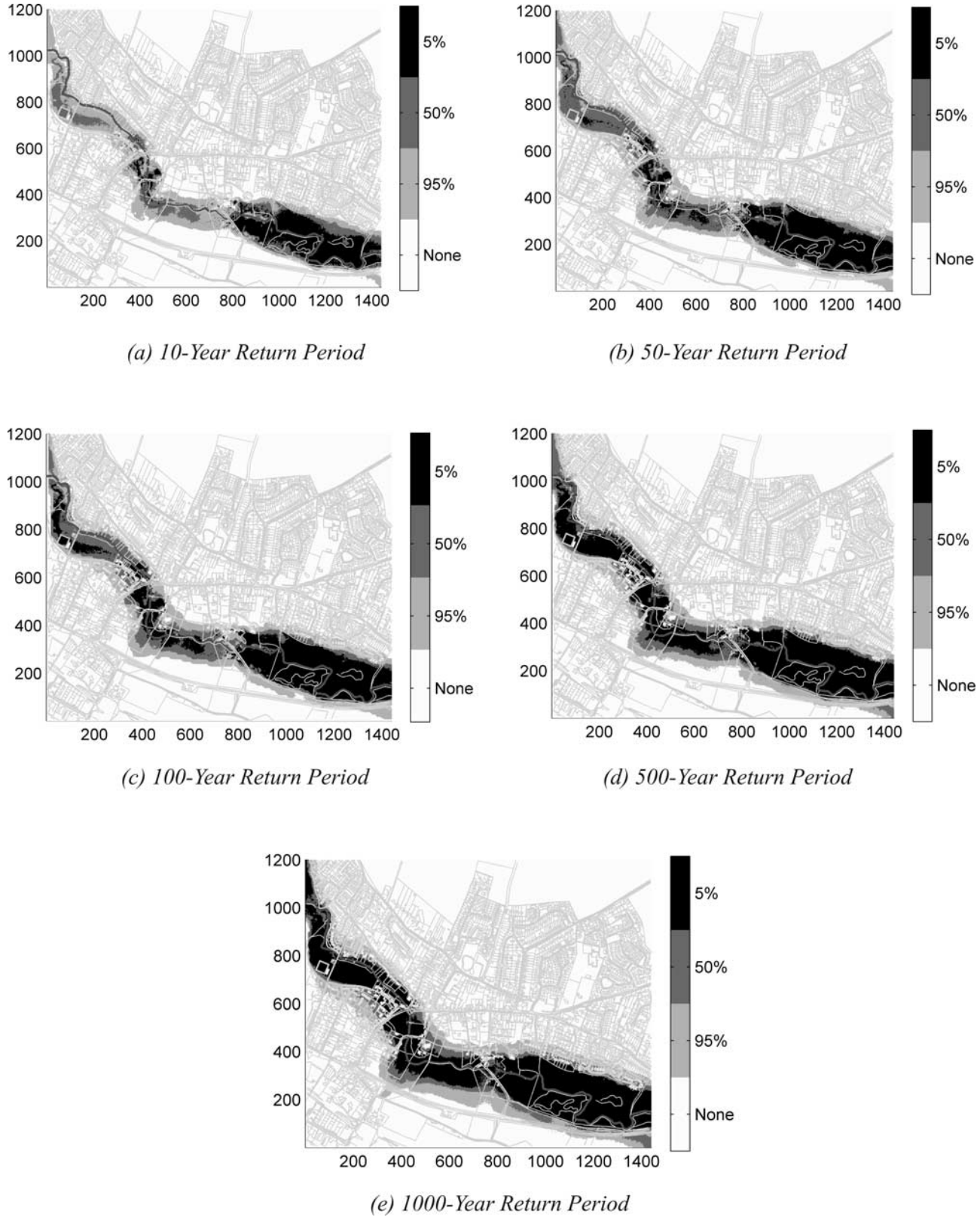

Figure 3. Areas of Predicted Inundation at the 5%, 50% and 95% points of the cumulative distribution of peak discharge magnitudes.

rainfall-runoff parameter set with the optimal value of the performance measure (Figure 6). This mimics the situation where there is no uncertainty in the rainfall-runoff model parameterization.

[49] In this situation, discharge estimate uncertainty is greatly reduced, e.g., the 90% confidence interval for the 100-year flood discharge is constrained from [14.8, 48.0] to [17.5, 20.8] $m^3 s^{-1}$, a significant advantage for any plan-

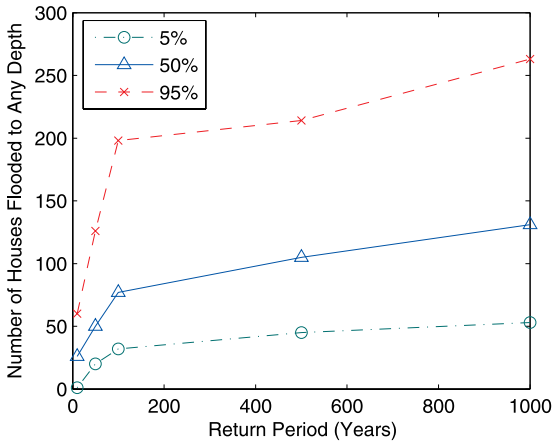

Figure 4. Number of houses flooded (to any depth) as a function of return period and point of peak discharge distribution.

ning of flood defense works. However, this analysis must not be confused with the results of using a single set of parameters without justification. Many of the alternative parameter sets had a performance value very close to the optimum, giving little reason to suppose that one set should be accepted against the rejection of all others. Discounting these other possible flow values may have particularly damaging consequences as the confidence limits fall at the lower end of the range of the wider bounds; the optimum set does not necessarily give values bracketing the median of the complete uncertainty analysis.

6.2. Propagating Uncertainty Through Inundation Simulations

[50] The preceding section analyzed the relative effects of uncertainty in the rainfall input and rainfall-runoff model parameters. To understand how such changes in discharge prediction distributions would affect inundation predictions in the coupled model structure, the uncertainty was propagated through the hydraulic model, as before (Figure 7). The 100-year event only was considered, as a standard for comparison.

[51] • Plot (a) shows the original analysis of the 100-year flood, repeated for comparison.

[52] • Plot (b) shows the significant reduction in uncertainty of flood boundary position possible if the rainfall-runoff model parameters could be defined exactly. Although this is unlikely due to equifinality in parameter sets, caused by model structural deficiencies and limited calibration data, it demonstrates that significant benefits could be achieved by further work to reduce the number of models considered behavioral.

[53] • Plot (c) shows the small reduction in uncertainty achievable if the future rainfall patterns were known exactly, however the relatively minor impact compared with that of Plot (b) suggests that improvements in rainfall-runoff modeling should take precedence over improvements in rainfall characterization.

6.3. Sensitivity to Inundation Model Parameterization

[54] As discussed, uncertainty in the channel friction parameter used to calibrate the floodplain inundation model was not considered due to computational constraints. However, a decoupled 'sensitivity analysis' was undertaken to assess the relative scale of this uncertainty.

[55] For each return period, the 50% (median) hydrograph was routed through the floodplain using channel friction coefficients of 0.04 and 0.06 $m^{-1/3}s$, chosen to surround the previously selected optimum of 0.05 $m^{-1/3}s$ which represented a single, global maximum in the validation statistic response space. More extreme values were found to depress validation scores. Inundation envelopes from the 100-year flood (Figure 8) show that varying the friction parameter value within the specified range has a relatively small effect relative to the uncertainty sources previously considered. It should however be understood that a simplistic analysis of this kind cannot represent the nonlinear effects of uncertainty propagation through the model chain, and hence provides only a guide as to the

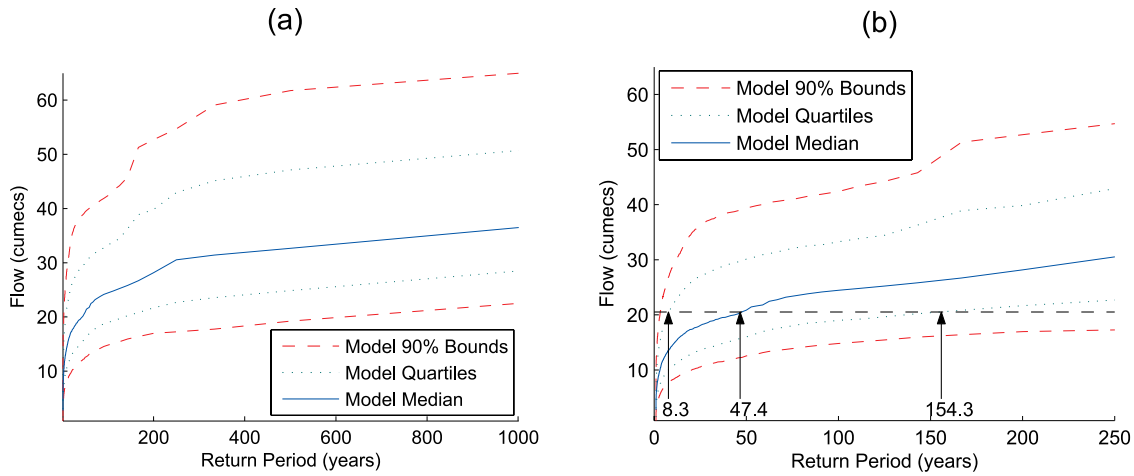

Figure 5. Modeled Discharge: Return Period Relation, using single rainfall series. (a) Full Range. (b) Detail. Dashed Line shows discharge associated with 2001 flood, with return period estimated from median and qu

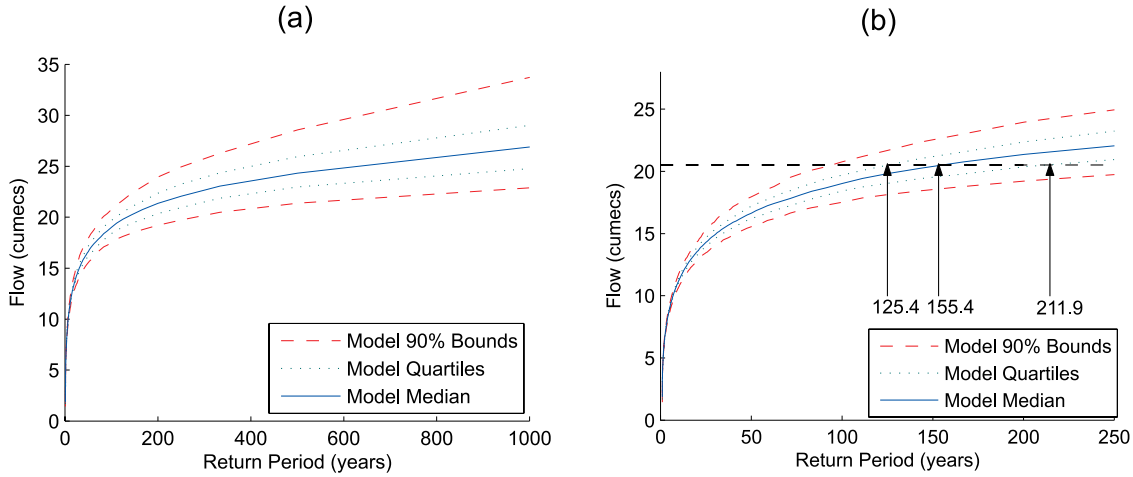

Figure 6. Modeled Discharge: Return Period Relation, using optimized rainfall-runoff model parameters. (a) Full Range. (b) Detail. Dashed Line shows discharge associated with 2001 flood, with return period estimated from median and quartiles.

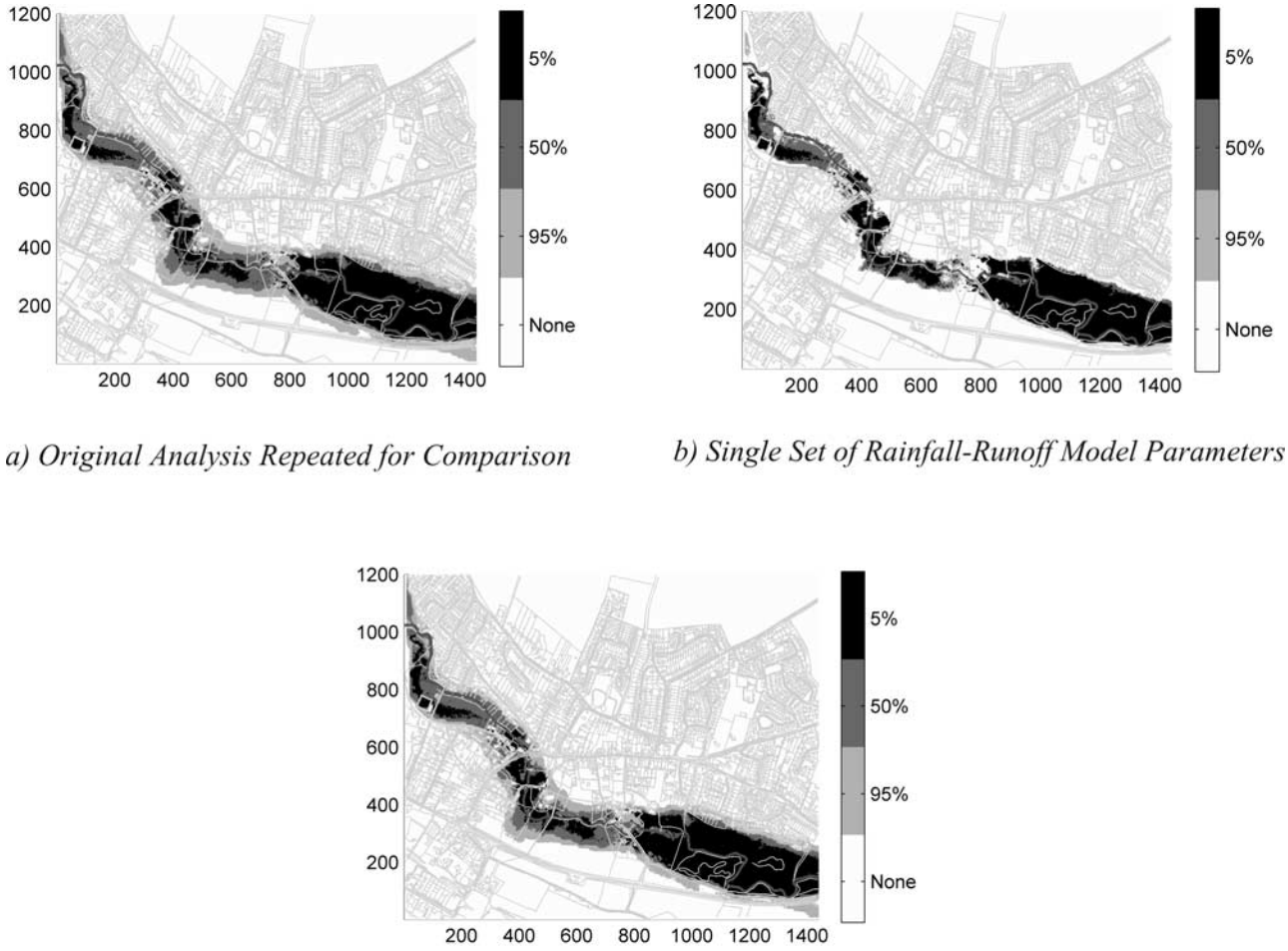

Figure 7. Areas of Predicted Inundation at the 5%, 50% and 95% points of the cumulative distribution of peak discharge magnitudes for the 100-year flood, using three alternative methods to calculate uncertainty boun

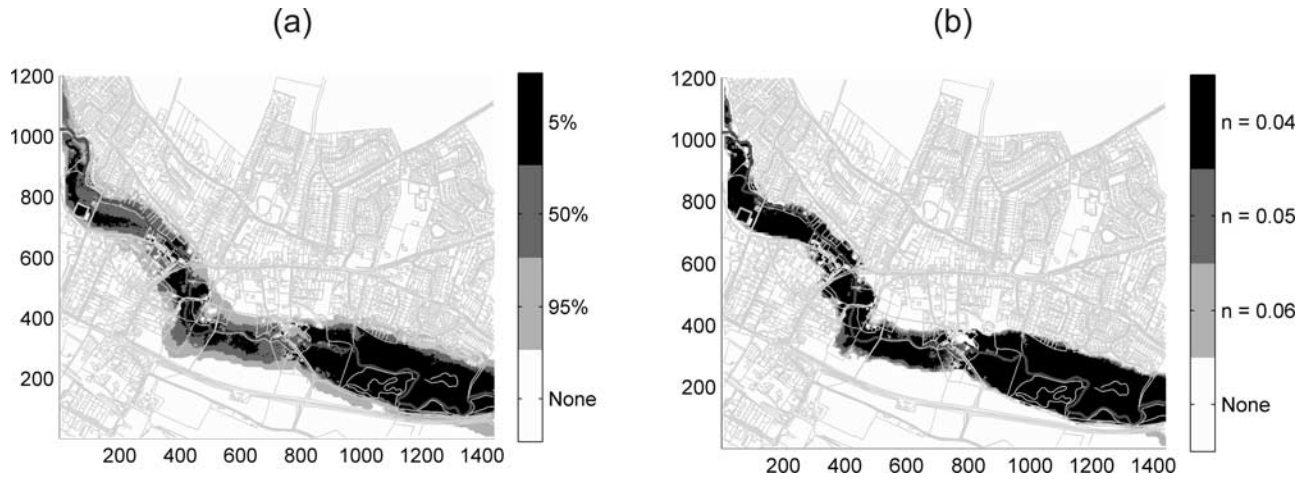

Figure 8. Variation in inundation envelope: Comparison of (a) Uncertainty in rainfall and rainfall-runoff model parameters and (b) Uncertainty associated with floodplain model channel friction parameter.

likely effect of uncertainty on model results in a full application of the GLUE procedure to the coupled model system.

7. Comparison With Standard Analysis

[56] To illustrate the characteristic differences of the End-to-End FRA framework from conventional methodologies, the inundation predictions made using the new method are compared with those of a standard FRA, carried out by the UK Environment Agency which is responsible for flood management at the trial site [*Bullen Consultants*, 2002; *Halcrow*, 2003, 2004]. The methods used are those currently recommended in the Flood Estimation Handbook [*Robson and Reed*, 1999]: a standard text which provides guidance widely used in planning scenarios and engineering applications. In brief, hydrographs are produced using a dual method. First, hydrograph shape is produced by routing a design rainfall event through a rainfall-runoff model. Five flood events during the period 2000–2001 are used to estimate the parameters of this model. Secondly, discharge magnitude is calculated using statistical methods. The discharge record is augmented using a 'pooling group analysis' which identifies hydrologically similar catchments based on catchment area, average annual rainfall and base flow regime; priority is given to catchments close to the study site. In the case of Linton, 17 other sites are used, giving a combined total of 486 years of record. Using this extended data set, the flood frequency curve is constructed by fitting a 3-parameter Generalized Logistic Distribution to the data, with cumulative distribution function as follows:

$$F(Q;k,\alpha,\xi) = \left[1 + \left(1 - \frac{k}{\alpha}(Q-\xi)^{1/k}\right)\right]^{-1} \qquad (k \neq 0) \quad (12)$$

The resulting discharge estimate is used to scale the hydrograph from the rainfall-runoff model. This provides an upstream boundary condition for a 1D hydraulic inundation model, based on cross-sectional data and created using ISIS modeling software (Wallingford Software Ltd, 2006), to route flow along the channel and overbank.

[57] The contrasting nature of the techniques is reflected in the predictions of the 100-year discharge: 10.2 $m^3 s^{-1}$ in the standard model versus 25.1 $m^3 s^{-1}$ median prediction in the end-to-end model, which manifest themselves in the inundation envelope forecasts (Figure 9). The difference stems from the constrained design event methodology of the standard analysis, such as an inability to include information on antecedent wetness conditions. However, most notable is an over-reliance on the gauged floodplain record in the statistical flood frequency analysis, which does not allow for measurement errors such as drowning of flow gauges during flood, as is known to happen at the trial site. In contrast, the end-to-end technique is able to compensate for such malfunctions using the correctly recorded rainfall data together with the calibrated rainfall-runoff model. This situation demonstrates the valuable way in which an integrated, end-to-end methodology can add value to short or censored methods by using models to capture information on physical catchment processes. In addition, a more complex pattern of inundation is predicted when using the new method with a 2D model, showing flow paths within the floodplain and high resolution definition of the flood boundary.

[58] The large difference in predictions of flood envelope has the potential to lead to very different approaches to flood risk mitigation. The representation of uncertainty within the end-to-end forecast also enables a more comprehensive consideration of possible flood scenarios which is not possible using the results of the standard analysis technique.

8. Discussion

[59] This paper set out to design a novel, flexible, process-based FRA methodology, relying on a chain of coupled models running within a proven uncertainty-estimation structure. A number of key findings are made. First, the benefits of extending the flood frequency analysis beyond discharge magnitude estimates to include inundation simulations were demonstrated. By integrating a hydraulic model into the coupled model cascade, hydrologists gain the opportunity to explore the relationships between discharge, inundation extent, flow paths, and likely damage to infrastructure and buildings. This is especially relevant in the light of recent trends away from

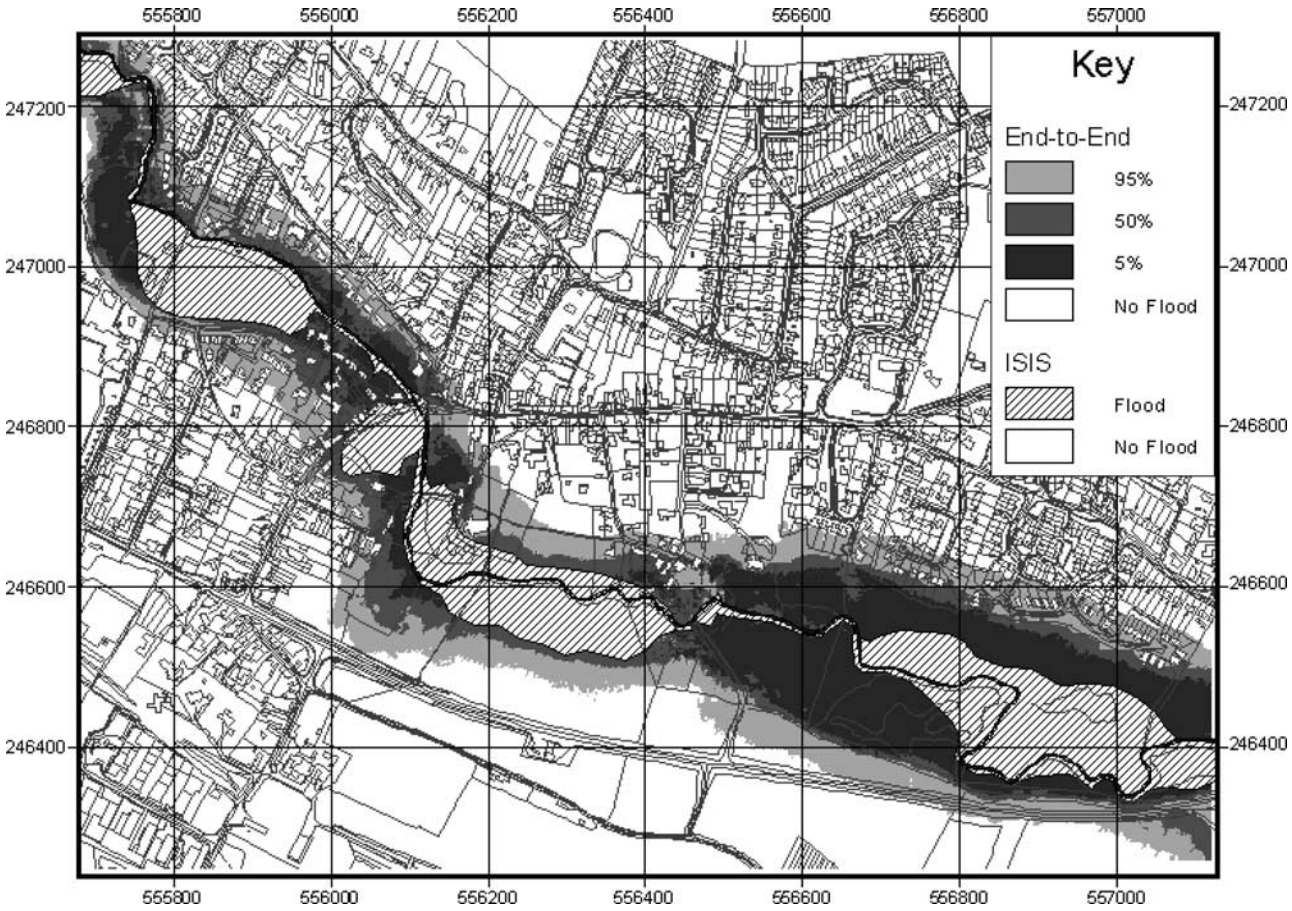

Figure 9. Comparison in 100-year flood envelopes predicted using the proposed End-to-End method versus a standard statistical method using the 1D ISIS flood model.

structural flood defences and toward a greater reliance on integrated catchment management approaches which aim to manage a 'functional floodplain'.

[60] An important aspect of the modeling procedure is the rejection of the principle of using deterministic forecasts. These are replaced by results in the form of distribution quantiles, which are presented as hazard maps to allow an intuitive interpretation of the effects of uncertainty on flood forecasts. Maps showing the confidence intervals allow an assessment of which areas of the floodplain are most sensitive to uncertainty in discharge predictions due to channel shape and local topography. Although the inclusion of uncertainty estimates in a flood frequency analysis is still a relatively rare occurrence outside academic research, its importance was demonstrated here: a deterministic model using a single set of rainfall-runoff model parameters was shown to give biased and under-predicted estimates of flood hazard. In this study, computational restraints forced a reduced set of hydraulic model simulations, however it is hoped that in the future the methodology could be extended to include uncertainty in hydraulic model parameterization as part of the full GLUE application. While it would not be practical to propagate predictions from each discharge series through the hydraulic model, a concept such as that of functional similarity [*Pappenberger et al.*, 2005] might be used to reduce computational effort. This complementary approach makes alternative choices to the method outlined here: rather than simplifying the coupling procedure between consecutive models, instead the number of rainfall-runoff model parameter sets is severely restricted, by classification according to the type of hydrograph forms produced.

[61] A wider reporting of the effects of uncertainty on model predictions may also provide an impetus for further data collection in order to constrain uncertainty. By emphasizing that observed floods may fall within wide prediction bounds rather than the more simplistic interpretation that the deterministic model is 'wrong', it becomes more obvious how additional data could aid future predictions. In this study, results showed that the major cause of uncertainty was equifinality in rainfall-runoff model parameterization, and therefore suggests that future effort might best be directed at reducing the range of behavior associated with the set of behavioral rainfall-runoff models. These more detailed conclusions are, however, dependant on the models and coupling methods chosen for the trial study, also the range of parameters and uncertainty sources that were analyzed.

9. Conclusion

[62] This paper presents the argument for process-based FRA methodology based on continuous simulation within the context of a chain of coupled models. Taking advantage of advances in data provision, and reduced complexity modeling techniques, high-resolution flood inundation simulation is included as part of the model chain. Such a

strategy is highly desirable in an age where non-stationarity of the flood generation process, together with changing approaches to flood mitigation, have rendered traditional statistical FRA techniques increasingly obsolete.

[63] Uncertainty estimation was included as an integral part of the procedure, to assess stochasticity and parameter uncertainty within the model chain. Results from a trial flood frequency analysis showed that significant uncertainty was present in estimates of flood extent, and indicated where future work might reduce this most effectively. The current use of deterministic flood risk analyses was found to be unduly restrictive and likely to give biased estimates of flood risk.

References

Antoniadis, A. (1995), Matlab Smoothing Toolbox, http://www.unizh.ch/biostat/Software/, Zurich.

Apel, H., A. H. Thieken, B. Merz, and G. Bloschl (2004), Flood risk assessment and associated uncertainty, *Nat. Hazards Earth Syst. Sci.*, *4*(2), 295–308.

Arnaud, P., and J. Lavabre (1999), Using a stochastic model for generating hourly hyetographs to study extreme rainfalls, *Hydrol. Sci. J.*, *44*(3), 433–446.

Arnell, N. W., and N. S. Reynard (1996), The effects of climate change due to global warming on river flows in Great Britain, *J. Hydrol.*, *183*(3–4), 397–424.

Arnell, N. W., C. Liu, R. Compagnucci, L. da Cunha, K. Hanaki, C. Howe, G. Mailu, and I. Shiklomanov (2001), *Climate Change 2001: Impacts, Adaptation and Vulnerability*, IPCC.

Aronica, G., P. D. Bates, and M. S. Horritt (2002), Assessing the uncertainty in distributed model predictions using observed binary pattern information within GLUE, *Hydrol. Processes*, *16*, 2001–2016.

Bates, P. D., and A. P. J. De Roo (2000), A simple raster-based model for flood inundation simulation, *J. Hydrol.*, *236*, 54–77.

Beven (1987), Towards the use of catchment geomorphology in flood frequency predictions, *Earth Surf. Processes Landforms*, *12*, 69–82.

Beven, K., and A. Binley (1992), The future of distributed models - model calibration and uncertainty prediction, *Hydrol. Processes*, *6*(3), 279–298.

Blazkova, S., and K. Beven (2002), Flood frequency estimation by continuous simulation for a catchment treated as ungauged (with uncertainty), *Water Resour. Res.*, *38*(8), 1139, doi:10.1029/2001WR000500.

Blazkova, S., and K. Beven (2004), Flood frequency estimation by continuous simulation of subcatchment rainfalls and discharges with the aim of improving dam safety assessment in a large basin in the Czech Republic, *J. Hydrol.*, *292*(1–4), 153–172.

Bullen Consultants (2002), Standard of protection studies, river Cam and Granta (Draft Report), Environment Agency, UK.

Cadavid, L., J. T. B. Obeysekera, and H. W. Shen (1991), Flood-frequency derivation from kinematic wave, *J. Hydraul. Eng.*, *117*(4), 489–510.

Cameron, D. S., K. J. Beven, and J. Tawn (1999), Flood frequency estimation by continuous simulation for a gauged upland catchment (with uncertainty), *J. Hydrol.*, *219*(3–4), 169–187.

Cameron, D. S., K. Beven, and J. Tawn (2000), An evaluation of three stochastic rainfall models, *J. Hydrol.*, *228*(1–2), 130–149.

Cernesson, F., J. Lavabre, and J. M. Masson (1996), Stochastic model for generating hourly hyetographs, *Atmos. Res.*, *42*(1–4), 149–161.

Chetty, K., and J. Smithers (2005), Continuous simulation modeling for design flood estimation in South Africa: Preliminary investigations in the Thukela catchment, *Phys. Chem. Earth*, *30*(11–16), 634–638.

Cunge, J. A., F. A. Holly Jr., and A. Verwey (1976), *Practical aspects of computational river hydraulics*, Pitman, London.

Dai, A., I. Y. Fung, and A. D. DelGenio (1997), Surface observed global land precipitation variations during 1900–88, *J. Clim.*, *10*(11), 2943–2962.

Dawson, R., J. Hall, P. Sayers, P. Bates, and C. Rosu (2005), Sampling-based flood risk analysis for fluvial dike systems, *Stochastic Environ. Res. Risk Assessment.*, *19*(6), 388–402.

De Roo, A. P. J., C. G. Wesseling, and W. P. A. Van Deursen (2000), Physically based river basin modelling within a GIS: The LISFLOOD model, *Hydrological*, *14*(11–12), 1981–1992.

De Roo, P. J., et al. (2003), Development of a European flood forecasting system, *Int. J. River Basin Manage.*, *1*(1), 49–59.

DEFRA (2002), *Flood Management - Capital Grant Allocations for Flood and Coastal Defence*, http://www.defra.gov.uk/environ/fcd/policy/grantaid.htm#scorecalc.

Diaz-Granados, M. A., J. B. Valdes, and R. L. Bras (1984), A physically based flood frequency distribution, *Water Resour. Res.*, *20*(7), 995–1002.

Eagleson, P. S. (1972), Dynamics of flood frequency, *Water Resour. Res.*, *8*(4), 878–898.

Easterling, D. R., et al. (2000), Observed variability and trends in extreme climate events: A brief review, *Bull. Am. Meteorol. Soc.*, *81*(3), 417–425.

Estrela, T., and L. Quintas (1994), Use of a GIS in the modelling of flows on floodplains, in *Proceedings of the* 2nd *International Conference on River Flood Dynamics*, edited by W. R. White and J. Watts, Wiley, Chichester.

Faulkner, D., and R. Wass (2005), Flood estimation by continuous simulation in the Don catchment, South Yorkshire, UK, *Water Environ. J.*, *19*(2), 78–84.

Franchini, M., A. M. Hashemi, and P. E. O'Connell (2000), Climatic and basin factors affecting the flood frequency curve: PART II - A full sensitivity analysis based on the continuous simulation approach combined with a factorial experimental design, *Hydrol. Earth Syst. Sci.*, *4*(3), 483–498.

Goel, N. K., R. S. Kurothe, B. S. Mathur, and R. M. Vogel (2000), A derived flood frequency distribution for correlated rainfall intensity and duration, *J. Hydrol.*, *228*, 56–67.

Groisman, P. Y., R. W. Knight, T. R. Karl, D. R. Easterling, B. M. Sun, and J. H. Lawrimore (2004), Contemporary changes of the hydrological cycle over the contiguous United States: Trends derived from in situ observations, *J. Hydrometeorol.*, *5*(1), 64–85.

Halcrow (2003), Audit of the Cam and Granta Hydraulic Model, Report, Environment Agency, UK.

Halcrow (2004), Rivers Cam and Granta Model Improvements: Model Construction and SOP Assessment, Final Report, Environment Agency, UK.

Hall, J. W., S. Tarantola, P. D. Bates, and M. S. Horritt (2005), Distributed sensitivity analysis of flood inundation model calibration, *J. Hydraul. Eng.*, *131*(2), 117–126.

Hashemi, A. M., M. Franchini, and P. E. O'Connell (2000), Climatic and basin factors affecting the flood frequency curve: PART I-A simple sensitivity analysis based on the continuous simulation approach, *Hydrol. Earth Syst. Sci.*, *4*(3), 463–482.

Hebson, C., and E. F. Wood (1982), A derived flood frequency distribution using Horton order ratios, *Water Resour. Res.*, *18*(5), 1509–1518.

Horritt, M. S., and P. D. Bates (2001), Predicting floodplain inundation: Raster-based modelling versus the finite-element approach, *Hydrol. Processes*, *15*(5), 825–842.

Hsieh, L. S., M. H. Hsu, and M. H. Li (2006), An assessment of structural measures for flood-prone lowlands with high population density along the Keelung River in Taiwan, *Natural Hazards*, *37*(1–2), 133–152.

Hunter, N. M., M. S. Horritt, P. D. Bates, and M. G. F. Werner (2004), Theoretical and practical limits to the use of storage cell codes for flood inundation modelling, in *Flood risk assessment*, edited by D. Reeve, Institute of Mathematics and its Applications, Southend-on-Sea.

Huntington, T. G. (2006), Evidence for intensification of the global water cycle: Review and synthesis, *J. Hydrol.*, *319*(1–4), 83–95.

Jakeman, A. J., I. G. Littlewood, and P. G. Whitehead (1990), Computation of the instantaneous unit hydrograph and identifiable component flows with application to two small upland catchments, *J. Hydrol.*, *117*, 275–300.

Kuchment, L. S., and A. N. Gelfan (2002), Estimation of extreme flood characteristics using physically based models of runoff generation and stochastic meteorological inputs, *Water Int.*, *27*(1), 77–86.

Kurothe, R. S., B. S. Goel, and N. K. Mathur (1997), Derived flood frequency distribution for correlated rainfall intensity and duration, *Water Resour. Res.*, *33*(9), 2103–2107.

Lamb, R. (1999), Calibration of a conceptual rainfall-runoff model for flood frequency estimation by continuous simulation, *Water Resour. Res.*, *35*(10), 3103–3114.

Maskey, S., V. Guinot, and R. K. Price (2004), Treatment of precipitation uncertainty in rainfall-runoff modelling: A fuzzy set approach, *Adv. Water Resour.*, *27*(9), 889–898.

McMillan, H. K. (2006), End-to-end flood risk assessment: A coupled model cascade with uncertainty estimation, Thesis, University of Cambridge.

McMillan, H. K., and J. Brasington (2007), Reduced Complexity Strategies for Modelling Urban Floodplain Inundation, *Geomorphology: In Press*. doi:10.1016/j.geomorph.2006.10.031.

Merz, B., H. Kreibich, A. Thieken, and R. Schmidtke (2004), Estimation uncertainty of direct monetary flood damage to buildings, *Natural Hazards Earth Syst. Sci.*, *4*(1), 153–163.

Nash, J. E. (1959), Systematic determination of unit hydrograph parameters, *J. Geophys. Res.*, *64*, 111–115.

Nash, J. E., and J. V. Sutcliffe (1970), River flow forecasting through conceptual models. 1. A discussion of principles, *J. Hydrol.*, *10*, 282–290.

Onof, C., D. Faulkner, and H. S. Wheater (1996), Design rainfall modelling in the Thames catchment, *Hydrol. Sci. J.-Journal Des Sciences Hydrologiques*, *41*(5), 715–733.

Osborn, T. J., and M. Hulme (2002), Evidence for trends in heavy rainfall events over the UK, *Phil. Trans. R. Soc. Ser. A*, *360*(1796), 1313–1325.

Pandit, A., and G. Gopalakrishnan (1996), Estimation of annual storm runoff coefficients by continuous simulation, *J. Irrig. Drain. Eng.*, *122*(4), 211–220.

Pappenberger, F., K. J. Beven, N. M. Hunter, P. D. Bates, B. T. Gouweleeuw, J. Thielen, and A. P. J. de Roo (2005), Cascading model uncertainty from medium range weather forecasts (10 days) through a rainfall-runoff model to flood inundation predictions within the European Flood Forecasting System (EFFS), *Hydrol. Earth Syst. Sci.*, *9*(4), 381–393.

Robson, A., and D. Reed (1999), Flood Estimation Handbook Volume 3: Statistical procedures for flood frequency estimation, Institute of Hydrology, Wallingford.

Romanowicz, R., and K. Beven (2003), Estimation of flood inundation probabilities as conditioned on event inundation maps, *Water Resour. Res.*, *39*(3), 1073, doi:10.1029/2001WR001056, 1061–1073.

Romanowicz, R., K. Beven, and J. Tawn (1996), Bayesian calibration of flood inundation models, in *Floodplain Processes*, edited by M. G. Anderson, D. E. Walling and P. D. Bates, Wiley, Chichester.

Sattler, K., and H. Feddersen (2005), Limited-area short-range ensemble predictions targeted for heavy rain in Europe, *Hydrol. Earth Syst. Sci.*, *9*(4), 300–312.

Sefton, C. E. M., and S. M. Howarth (1998), Relationships between dynamic response characteristics and physical descriptors of catchments in England and Wales, *J. Hydrol.*, *211*, 1–16.

Silverman, B. W. (1982), Kernel density estimation using the fast Fourier transform, *J. R. Stat. Soc. Ser.*, *31*(1), 93–99.

Silverman, B. W. (1986), *Density estimation for statistics and data analysis. Monographs on statistics and applied probability*, Chapman and Hall, London.

Staeger, T., J. Grieser, and C. D. Schonwiese (2003), Statistical separation of observed global and European climate data into natural and anthropogenic signals, *Clim. Res.*, *24*(1), 3–13.

US Army Corps of Engineers (2005), *HEC History*, http://www.hec.usace.army.mil/whoweare/history.html.

Walshaw, D. (1994), Getting the most from your extreme wind data: A step-by-step guide, *J. Res. Natl. Inst. Stand. Technol.*, *99*(4), 399–411.

Woolhiser, D. A., and J. A. Liggett (1967), Unsteady, one-dimensional flow over a plane- The rising hydrograph, *Water Resour. Res.*, *3*, 753–771.

Wheater, H. S. (2006), Flood Risk and Flood Management, *Phil. Trans. R. Soc. Lond. A*, In Press.

Young, P. C. (2003), Top-down and data-based mechanistic modelling of rainfall-flow dynamics at the catchment scale, *Hydrol. Processes*, *17*, 2195–2217.

Young, P. C., and K. Beven (1991), Computation of the instantaneous unit hydrograph and identifiable component flows with application to two small upland catchments - Comment, *J. Hydrol.*, *129*(1–4), 389–396.

Young, P. C., and K. Beven (1994), Data-based mechanistic modeling and the rainfall-flow nonlinearity, *Environmetrics*, *5*(3), 335–363.

Yu, D., and S. N. Lane (2006), Urban fluvial flood modelling using a two-dimensional diffusion-wave treatment, part 2: Development of a sub-grid-scale treatment, *Hydrol. Processes*, *20*(7), 1567–1583.

J. Brasington, Centre for Catchment and Coastal Research, University of Wales, Aberystwyth, SY23 3DB, UK.

H. K. McMillan, National Institute of Water and Atmospheric Research Ltd, 10 Kyle St, PO Box 8602, Riccarton, Christchurch, New Zealand. (h.mcmillan@niwa.co.nz)